East European Journal of Physics. 3. 226-235 (2024)
DOI:10.26565/2312-4334-2024-3-22 ISSN 2312-4334

FLOW OF MAGNETOHYDRODYNAMIC MAXWELL FLUID IN DARCY – FORCHHEIMER MODEL, WITH CATTANEO – CHRISTOV HEAT FLUX, OVER A STRETCHING SHEET SUBJECTED TO CONVECTIVE BOUNDARY CONDITIONS

D. Dastagiri Babu[a]*, S. Venkateswarlu[a], R. Hanuma Naik[b], D. Manjula[c]
[a]*Department of Mathematics, Rajeev Gandhi Memorial College of Engineering and Technology, Nandyal-518501, Andhra Pradesh, India*
[b]*Department of Electronics and Communication Engineering, Rajeev Gandhi Memorial College of Engineering and Technology, Nandyal-518501, Andhra Pradesh, India*
[c]*Department of Mathematics, Mother Theresa Institute of Engineering and Technology, Palamaner-517408, Andhra Pradesh, India*
**Corresponding Author e-mail: dastagiri478@gmail.com*
Received May 18, 2024; revised July 8, 2024; accepted July 12, 2024

This research communication explores the Darcy - Forchheimer flow of a chemically reacting non-Newtonian Maxwell fluid over a stretching sheet, incorporating the Cattaneo – Christov heat flux under a convective boundary condition. The fluid flow is described by a set of partial differential equations, which are subsequently transformed into a system of nonlinear ordinary differential equations. To solve these equations numerically, the BVP4C Method was employed after appropriately defining non dimensional variables and implementing similarity transformations. The impacts of diverse active parameters such as Deborah parameter, Darcy-Forchheimer parameter, magnetic parameter, Biot number, and porous parameter are examined on the velocity, temperature, and concentration profiles. In addition, the value of the Skin friction, Nusselt number is calculated and presented through tabular forms.
Keywords: *MHD; Maxwell fluid; Darcy-Forchheimer model; Cattaneo-Christov heat flux; Magnetic parameter*
PACS: 44.05.+e, 44.30.+v, 47.11.-j, 44.40.+a, 47.70.Fw

INTRODUCTION

As Advancements in technology progress, our understanding of fluid dynamics has expanded beyond the limitations of Newtonian models. The emergence of non-Newtonian fluid concepts has proven invaluable in comprehending complex flow behaviors. Of particular interest is the Maxwell fluid, renowned for its remarkable attributes in both technical and industrial applications. Maxwell fluids are employed to enhance the thermal radiation characteristics of conductive fluids. In the polymer manufacturing industry, they are particularly useful for understanding and controlling the flow behavior of polymer melts during processing, as well as for optimizing thermal properties such as heat transfer and radiation. Additionally, Maxwell fluids play a role in modeling the behavior of biological fluids, such as blood flow in arteries, where both elastic and viscous effects are significant.

Khan et al. [1] conducted a study on the mathematical analysis of heat and mass transfer in a Maxwell fluid flowing over a stretching sheet, considering the influence of thermophoretic and stratification effects. The heat transport within a two-dimensional steady radiative boundary layer involving Maxwell fluid flow, while also analyzing the impact of heat generation nd Magnetohydrodynamics (MHD) over a porous inclined plate investigated by Sudarmozhi *et al*. [2]. Zhao *et al*. [3] reported the study of unsteady natural convection heat and mass transfer in a porous medium involving a fractional MHD Maxwell fluid, considering the presence of Soret and Dufour effects. Hayat *et al*. [4] analyzed the heat and mass transfer analysis in the stagnation region of Maxwell fluid with chemical reaction over stretched surface. In their study, Riaz *et al*. [5] focused on the combined effects of heat and mass transfer on MHD free convective flow of Maxwell fluid with variable temperature and concentration. The numerical analysis of absorbing boundary condition for the Maxwell fluid flow over a semi-infinite plate with considering the magnetic field was studied by Bao *et al*. [6]. Yasin *et al*. [7] discussed a contemporary investigation on peristatically induced flow of Maxwell fluid, incorporating the modified Darcy's law and Hall effect alongside slip conditions. Babu *et al*. [8] focused on numerical investigation of Thermophorosis and activation energy effects of Maxwell nano fluid over an inclined magnetic field applied to a disk. The authors [9,10,11,12] have instigated the MHD flow and Heat transfer for Maxwell fluid over an exponentially stretching sheet with variable thermal conductivity in porous medium.

Darcy-Forchheimer flow characterizes the movement of fluid through a porous substance, combining the principles of Darcy's law and Forchheimer's quadratic resistance law. This phenomenon finds widespread application in engineering and geophysics, including scenarios like ground water percolation through soil, oil seepage in porous rock formations, and fluid passage within packed beds in chemical reactors. Darcy's law fundamentally states that the flows rate of a fluid through a porous material is directly proportional to the pressure gradient. This principle serves as a cornerstone in understanding fluid movement in porous media.

In their study, Waqas et al. [13] delved into the properties of Magneto-Maxwell nano lquid towards moving radiated surface. Flow analysis subject to Darcy-Forchheimer concept is studied. Newtonian heat/mass conditions and

Cite as: D.D. Babu, S. Venkateswarlu, R.H. Naik, D. Manjula, East Eur. J. Phys. 3, 226 (2024), https://doi.org/10.26565/2312-4334-2024-3-22

heat source aspects are taken into account for modeling. Rashid et al. [14] explored the Darcy-Forchheimer flow of Maxwell fluid with activation energy and thermal radiation over an exponential surface. Upreti et al. [15] analyzed the computational study on MHD Darcy-Forchheimer flow and double-diffusive modeling of Maxwell fluid over rotating stretchable surface. Das et al. [16] and Ganesh et al. [17] studied on the Darcy Forchheimer flow of hydromagnetic fluid flow over a stretching surface in a thermally stratified porous medium with second order slip, viscous and ohmic dissipation effects. Cui et al. [18] developed the thermal analysis of radiative Darcy-Forchheimer nano fluid flow across an inclined stretching surface.

The Cattaneo-Christov heat flux model improves upon Fourier's law of heat conduction by incorporating a finite thermal relaxation time, enhancing accuracy for systems with notable thermal inertia or fast temperature variations. This model, when coupled with MHD Maxwell fluids, characterizes visco-elastic fluids affected by magnetic fields and transient heat transfer. Its application extends to analyzing phenomena such as the flow of electrically conducting fluid in magnetic confinement fusion, behavior of magnetorheological fluids in magnetic fields, and heat transfer in systems experiencing rapid temperature changes or possessing high conductivity. Jawad and Nisar [19] studied the upper convected flow of Maxwell fluid near stagnation point through porous surface using heat flux model. Khan et al. [20] developed the numerical investigation of MHD Cattaneo-Christov thermal flux frame work for Maxwell fluid over a steady extending surface with thermal generation in a porous medium. Rubab and Mustafa [21] conducted a study on the MHD three-dimensional upper-convected Maxwell fluid over a bi-directional stretching surface by considering the Cattaneo-Christov heat flux model. The numerical study of radiative Maxwell viscoelastic magnetized flow from a stretching permeable sheet with a Cattaneo-Christov heat flux was developed by Sahid et al. [22]. Islam et al. [23] studied the Cattaneo-Christov theory for a time-dependent magnetohydrodynamics Maxwell fluid through a stretching cylinder. Salmi et al. [24] explained the numerical study of heat and mass transfer enhancement in Prandtl fluid MHD flow using Cattaneo-Christov heat flux theory.

The current study delves into the investigation of steady, two-dimensional flow of a Darcy-Forchheimer Maxwell fluid through a stretchable surface. Additionally, the analysis incorporates heat and mass transfer phenomena, employing the Cattaneo-Christov theory with chemical reactions. The novelty of this work lies in its examination of the Darcy-Forchheimer Maxwell fluid within the framework of the Cattaneo-Christov theory, considering convective boundary conditions, a combination not explored in existing literature. To address this gap, the authors undertake an examination of such effects on Maxwell fluid flow. To normalize the system, similarity variables are introduced. Numerical solutions are obtained using the Matlab bvp4c technique. The study discusses the graphical representation of the evolving parameters along the velocity profile, temperature profile, and concentration profile.

FORMULATION

Figure 1 illustrates a MHD steady Darcy – Forchheimer flow of Maxwell fluid. An incompressible fluid saturates the porous plate. Flow is caused due to a linear stretching surface. Cattaneo-Christov heat flux model instead of conventional Fourier's law of heat conduction is applied to study the heat transfer characteristics. The Cartesian coordinate system is adopted in such a way that x-axis is taken along the stretching sheet and y-axis is orthogonal to it.

Let $U_w(x) = ax$ denotes the surface stretching velocity along the x-axis direction. We also consider the effect of constant magnetic field of strength B_0 which is applied normally to the sheet. With these assumptions, the governing equations for continuity, velocity, temperature, and concentration in a steady two dimensional flow of a Maxwell fluid are given by

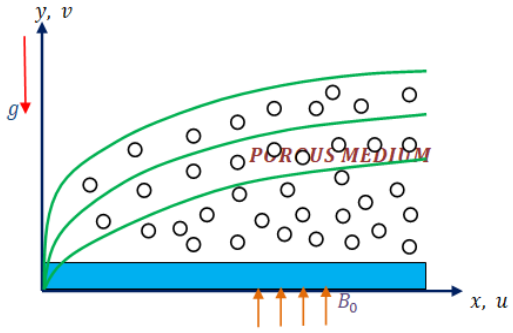

Figure 1. Schematic diagram

$$\frac{\partial u}{\partial x}+\frac{\partial u}{\partial y}=0 \tag{1}$$

$$u\frac{\partial u}{\partial x}+v\frac{\partial u}{\partial y}+\lambda_1\left[u^2\frac{\partial^2 u}{\partial x^2}+v^2\frac{\partial^2 u}{\partial x^2}+2uv\frac{\partial^2 u}{\partial x\partial y}\right]=\nu\frac{\partial^2 u}{\partial y^2}-\frac{\nu}{k}u-Fu^2-\frac{\sigma {B_0}^2}{\rho}u \tag{2}$$

$$u\frac{\partial T}{\partial x}+v\frac{\partial T}{\partial y}+\lambda_2\left[\begin{array}{l} u\dfrac{\partial u}{\partial x}\dfrac{\partial T}{\partial x}+v\dfrac{\partial v}{\partial y}\dfrac{\partial T}{\partial y}+u\dfrac{\partial v}{\partial x}\dfrac{\partial T}{\partial y} \\ +v\dfrac{\partial u}{\partial y}\dfrac{\partial T}{\partial x}+2uv\dfrac{\partial^2 T}{\partial x\partial y} \\ +u^2\dfrac{\partial^2 T}{\partial x^2}+v^2\dfrac{\partial^2 T}{\partial y^2} \end{array}\right]=\alpha\frac{\partial^2 T}{\partial y^2}+\frac{\sigma {B_0}^2}{\rho c_p}u^2+\tau\left[\begin{array}{l} D_B\dfrac{\partial C}{\partial y}\dfrac{\partial T}{\partial y} \\ +\left(\dfrac{D_m}{T_\infty}\right)\left(\dfrac{\partial T}{\partial y}\right)^2 \end{array}\right] \tag{3}$$

$$u\frac{\partial C}{\partial x}+v\frac{\partial C}{\partial y}=D_B\frac{\partial^2 C}{\partial y^2}+\left(\frac{D_m}{T_\infty}\right)\frac{\partial^2 T}{\partial y^2}-K_r\left(C-C_\infty\right) \tag{4}$$

With boundary conditions

$$\left.\begin{array}{l} u=u_w(x)=ax,\quad v=0,\quad -k\dfrac{\partial T}{\partial y}=h_f\left(T_f-T\right),\ C=C_w\,at\quad y=0 \\ u\to 0,\ T\to T_\infty,\ C\to C_\infty\quad as\quad y\to\infty \end{array}\right\} \tag{5}$$

Invoking the following similarity transformations

$$u=axf'(\eta);\quad v=-\sqrt{ax}f(\eta);\ \theta(\eta)=\frac{T-T_\infty}{T_f-T_\infty};\quad \eta=y\sqrt{\frac{a}{\upsilon}};\ \phi(\eta)=\frac{C-C_\infty}{C_f-C_\infty}; \tag{6}$$

Equation (1) is identically satisfied and Equations (2), (3), (4), and (5) with the help of Equation (6) take the following forms:

$$f'''+ff''+\beta\left(2ff'f''-f^2f'''\right)-\lambda f'-F_r\left(f'\right)^2-Mf'=0 \tag{7}$$

$$\theta''+EcPrM\left(f'\right)^2+\Pr Nb\theta'\phi'+PrNt\left(\theta'\right)^2-Prf\theta'-\Gamma Pr\left(ff'\theta'+f^2\theta''\right)=0 \tag{8}$$

$$\phi''+fSc\phi'+\left(\frac{Nt}{Nb}\right)\theta''-KcSc\phi=0 \tag{9}$$

The transformed boundary conditions are

$$\left.\begin{array}{l} At\ \eta=0,\ f=0,\ f'=1,\ \theta'=-Bi\left[1-\theta\right],\ \phi'=1 \\ As\ \eta\to\infty,\ f'\to 0,\ \theta'\to 0,\ \phi\to 0 \end{array}\right\} \tag{10}$$

Where β is the Deborah number, $\Gamma=\lambda_2 a$ is the non-dimensional thermal relaxation time, $\lambda=\dfrac{\nu}{ka}$ denotes the porosity parameter, $Fr=\dfrac{Cb}{\sqrt{k}}$ represents the inertia coefficient, Cb represents drag coefficient, $Pr=\dfrac{\nu}{\alpha}$ stands for Prandtl number, $M=\dfrac{\sigma {B_0}^2}{\rho a}$ is the magnetic parameter, $Sc=\dfrac{\nu}{D_B}$ denotes Schmidt number, $Kc=\dfrac{Kr}{a}$ represents the chemical reaction parameter, $Nt=\dfrac{\tau D_B\left(T_f-T_\infty\right)}{\nu T_\infty}$ is the Thermophoretic parameter, $Nb=\dfrac{\tau D_B\left(C_f-C_\infty\right)}{\nu}$ denotes Brownian motion parameter, $Bi=\sqrt{\dfrac{\nu}{a}}\left(\dfrac{h_f}{k}\right)$ represents the Biot number, λ_2 denotes Relaxation time for heat flux.

The expression for the Local Skin friction, the Local Nusselt number, and the Sherwood number are defined as:

$$C_f{Re_r}^{1/2}=f''(0);\quad Nu{Re_r}^{-1/2}=-\theta'(0);\quad Sh{Re_r}^{-1/2}=-\phi'(0);$$

METHODOLOGY

The reduced ODE models (7), (8), and (9) are solved numerically by applying the MATLAB bvp4c algorithm. In this regard, initially we convert the higher order equations to first order equations. Let us

take $f_1 = f, f_2 = f', f_3 = f'', f_4 = \theta, f_5 = \theta', f_6 = \phi, f_7 = \phi'$ .Then the reduced equations are written as in the following form:

$$f_1' = f_2 \tag{11}$$

$$f_2' = f_3 \tag{12}$$

$$f_3' = \frac{1}{\left(1-\beta f_1^2\right)}\left(\lambda f_2 + Frf_2^2 + Mf_2 - f_1 f_3 - 2\beta f_1 f_2 f_3\right) \tag{14}$$

$$f_4' = f_5 \tag{15}$$

$$f_5' = \frac{1}{\left(1-\Gamma \Pr f_1^2\right)}\left(\Gamma \Pr f_1 f_2 f_5 + \Pr f_1 f_5 - Ec \Pr Mf_2^2 - \Pr Nbf_5 f_7 - \Pr Ntf_5^2\right) \tag{16}$$

$$f_6' = f_7 \tag{17}$$

$$f_7' = KcScf_6 - Scf_1 f_7 - \frac{Nt}{Nb}\left(\Gamma \Pr f_1 f_2 f_5 + \Pr f_1 f_5 - Ec \Pr Mf_2^2 - \Pr Nbf_5 f_7 - \Pr Ntf_5^2\right) \tag{18}$$

The transformed boundary conditions are

$$\left.\begin{aligned} &At\ \eta = 0,\ f_1 = 0,\ f_2 = 1,\ f_5 = -Bi\left[1 - f_4\right],\ f_7 = 1 \\ &As\ \eta \to \infty,\ f_2 \to 0,\ f_5 \to 0,\ f_6 \to 0 \end{aligned}\right\} \tag{19}$$

RESULTS AND DISCUSSIONS

In this study, a system of nonlinear ordinary differential equations represented by the equations (7), (8), and (9), subject to the constraints specified in equation (10), is solved numerically. The numerical solution is obtained using the shooting process with the bvp4c MATLAB Package. This computational approach allows for the investigation of the influence of various non-dimensional parameters on the profiles of velocity, temperature, and concentration within the system.

Specially, the study explores the impact of non-dimensional parameters such as Deborah number, inertia coefficient, and Biot number, and others on the velocity, temperature and concentration profiles. Additionally, the effects of these parameters on skin friction coefficient, Nusselt number are examined. The study maintains certain non-dimensional parameter values throughout its analysis, setting M to 0.5, Pr to 0.62, Bi to 0.7, Ec to 1, Nt to 0.3, Nb to 0.3, Fr to 0.5, and β to 0.2, λ to 0.2. These values remain constant through the study, except when varying parameters are explicitly depicted in the figures. Overall, the study provides valuable insights into the behavior of the system under different parameter combinations, facilitating a deeper understanding of the underlying physical phenomena and aiding in the optimization of system performance.

Figures 2-4 illustrates the impact of the local Forchheimer number (inertia coefficient) Fr. It is evident from the figures that fluid velocity diminishes with enhancing Fr, as the inertia coefficient is directly related to the porosity of the medium and drag coefficient Cb. Thus, with higher values of Cb, both the porosity of the medium and drag coefficient enhances. Consequently, the resistance force on the liquid is enhanced, resulting in lower velocity corresponding to larger Forchheimer numbers. An enhancing in inertia coefficient (Fr) leads to stronger temperature and concentration profiles and more thickness of boundary layers.

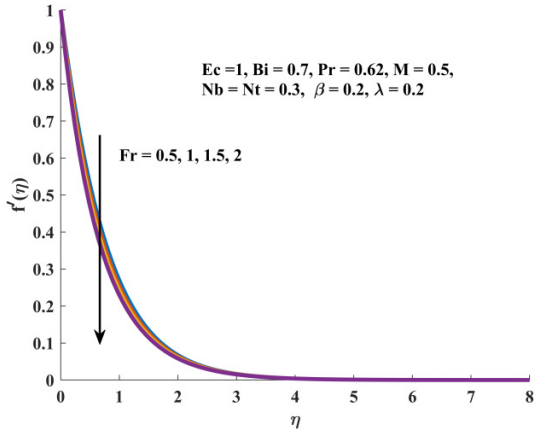

Figure 2. Sketch of Fr on f'

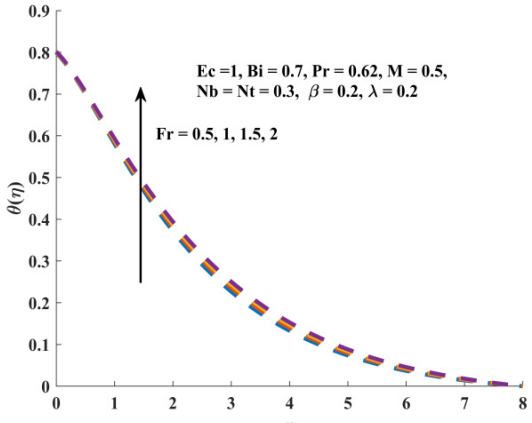

Figure 3. Sketch of Fr on θ

Figures 5–7 depicts the change in velocity, concentration, and temperature profiles for different values of the porosity parameter λ. As porous media tends to increase resistance to fluid motion, the fluid velocity diminishes accordingly. Conversely, an opposite trend is observed in the concentration profile and temperature profile with an increase in the porosity parameter.

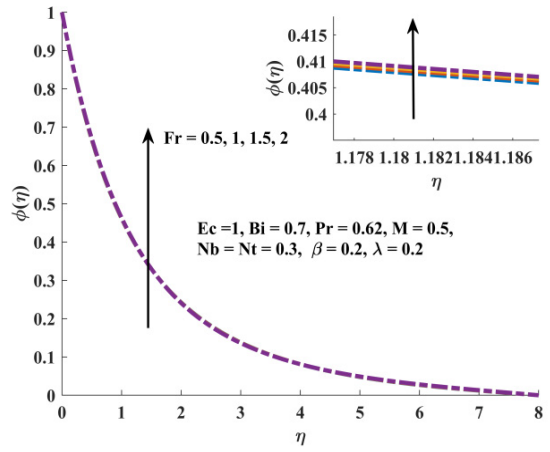

Figure 4. Sketch of Fr on ϕ

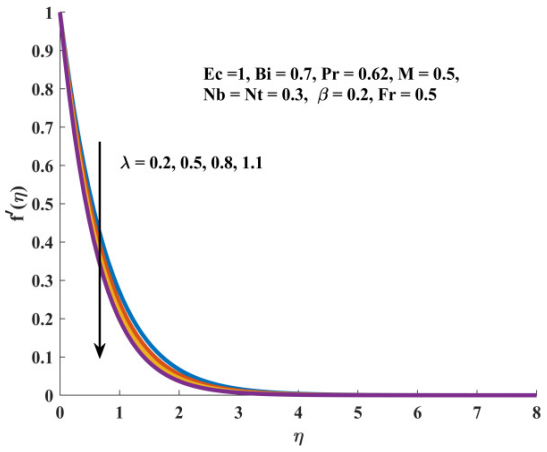

Figure 5. Sketch of λ on f'

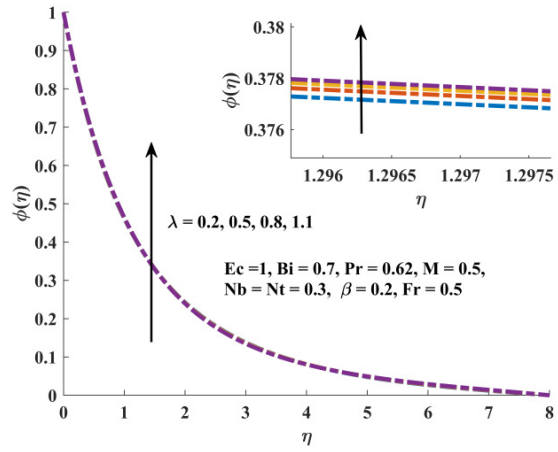

Figure 6. Sketch of λ on ϕ

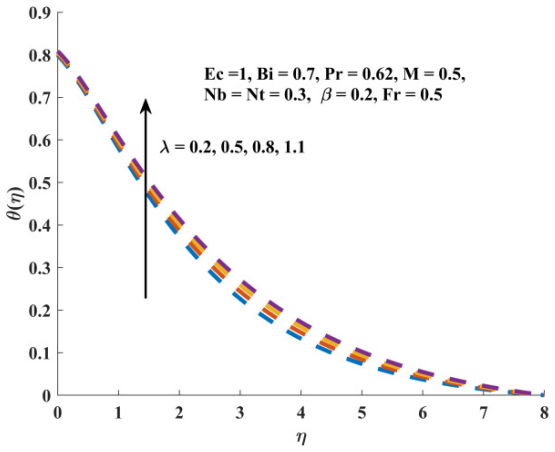

Figure 7. Sketch of λ on θ

Figures 8-10 elucidate how the imposition of magnetic constraints (M) impacts velocity, temperature, and concentration fields. Analysis of these figures led us to anticipate a flattening of fluid velocity with enhancing M. Physically, the magnetic field induces a drag force that opposes fluid motion, thereby reducing velocity. Conversely, temperature and species concentration profiles intensify with changes in the magnetic parameter.

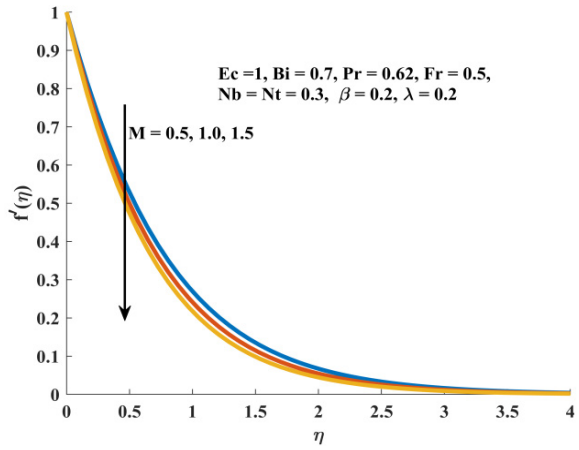

Figure 8. Sketch of M on f'

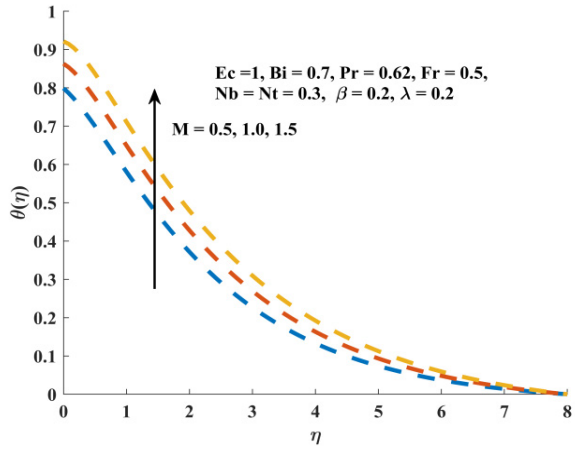

Figure 9. Sketch of M on θ

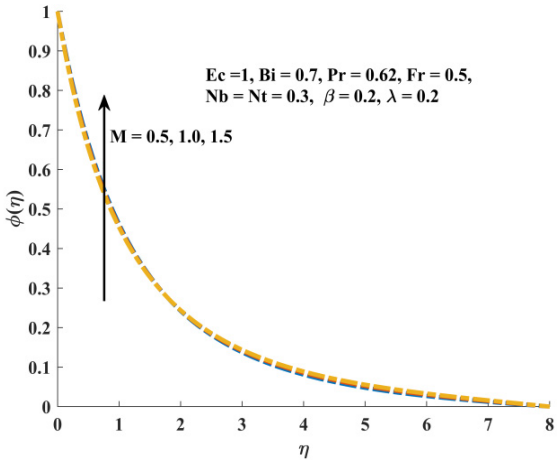

Figure 10. Sketch of M on ϕ

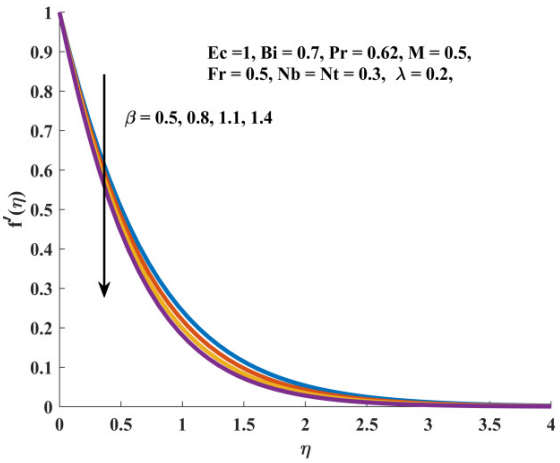

Figure 11. Sketch of β on f'

Figure 11 illustrates how the velocity distribution $f'(\eta)$ is influenced by the Deborah number. As the Deborah number (β) enhances, resulting that the velocity diminishes. In Figure 12, it is shown that higher values of the Deborah number lead to an augmentation in the temperature field (θ) and thickness of the thermal boundary layer. Physically, the Deborah number is associated with relaxation time, which is greater for higher Deborah numbers. Consequently, a larger relaxation time correlates with higher temperatures and thicker thermal boundary layers. The impact of Deborah number (β) on the concentration profile is depicted in Figure 13. Here we observed that the concentration profile is higher when we enhance the values of Deborah number (β).

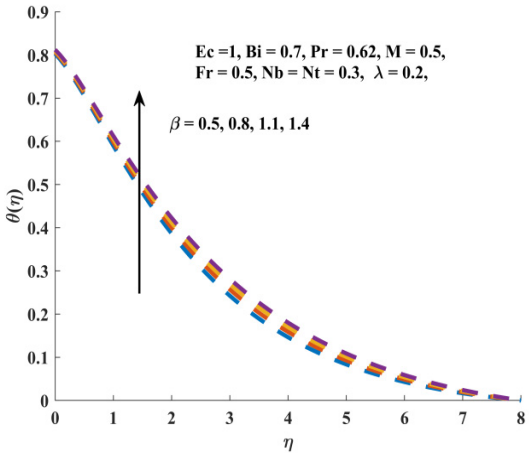

Figure 12. Sketch of β on ϕ

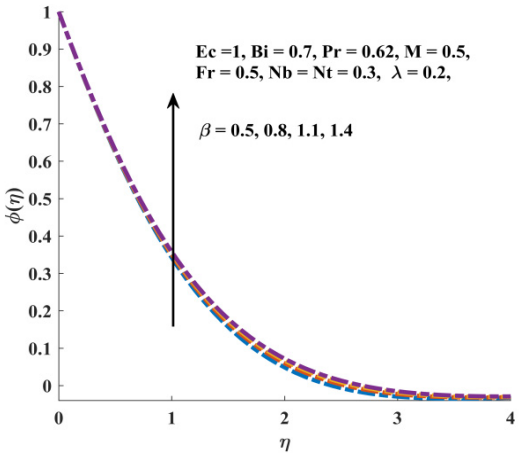

Figure 13. Sketch of β on θ

Observing the Figure 14, it becomes apparent that the temperature profile of the fluid diminishes as the thermal relaxation parameter (Γ) enhances. This phenomenon occurs because, as the parameter (Γ) rises, material particles require more time to transfer heat to adjacent particles. In essence, for higher values of the thermal relaxation parameter (Γ), the material exhibits characteristics akin to non-conductivity, leading to decrease in the temperature profile. Consequently, it can be concluded that the temperature profile is lower in the case of the Cattaneo-Christov heat flux model compared to Fourier's Law. Figure 15 describes the impact of thermal relaxation parameter (Γ) on concentration profile. It shows an increase in the thermal relaxation parameter, the concentration distribution also enhances.

Figures 16-17 showcase the influence of the Prandtl number (Pr) on temperature and concentration distribution. The Prandtl number varies depending on the material and is unique to each fluid. The figures indicate that as Pr increases, the fluid temperature decreases. A high Pr implies that momentum diffusivity surpasses thermal diffusivity, resulting in a reduction in energy boundary layer thickness. Typically, in heat transfer problems, Pr is employed to decrease the relative thickness of both thermal and momentum boundary layers. Similarly, this behavior is observed in concentration profiles.

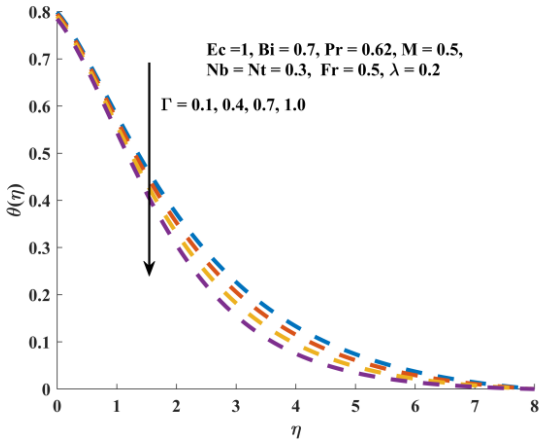

Figure 14. Sketch of Γ on θ

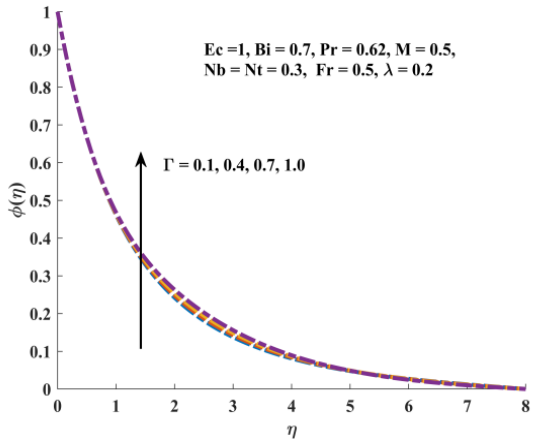

Figure 15. Sketch of Γ on ϕ

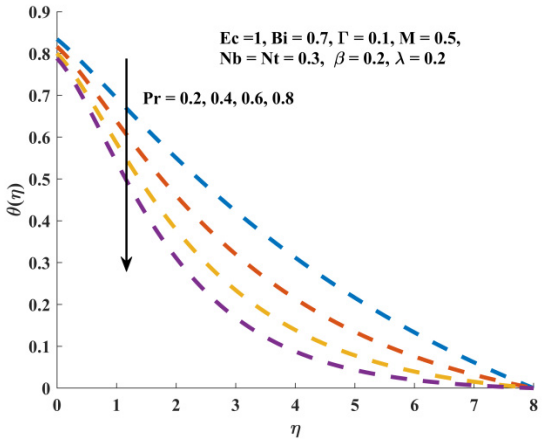

Figure 16. Sketch of Pr on θ

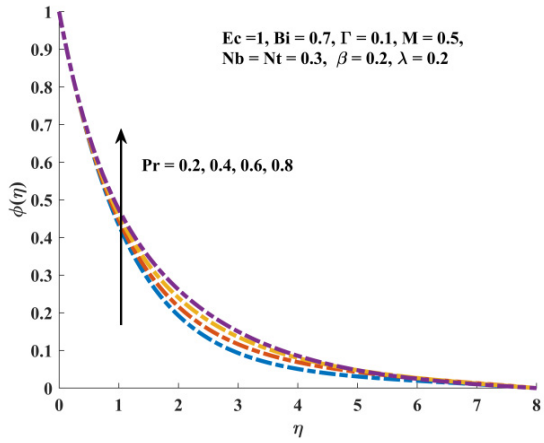

Figure 17. Sketch of Pr on ϕ

Figures 18-19 depict the impact of the thermophoresis parameter (Nt) on the both temperature profiles and concentration profiles. These figures depict that $\theta(\eta),\phi(\eta)$ are the increasing function of thermophoresis parameter for escalating values of Nt. As Nt increases, the thermal conductivity of liquid also enhances. A higher thermal conductivity liquid leads to more advanced temperature and concentration fields.

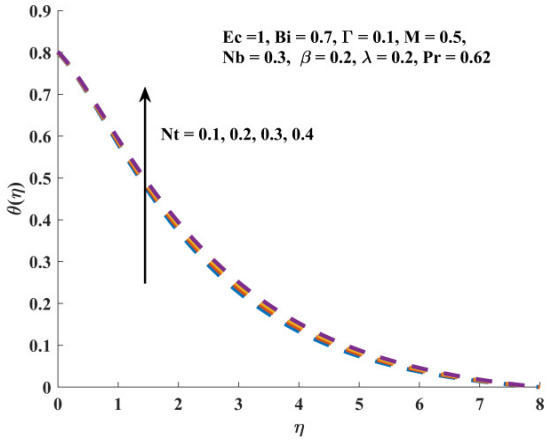

Figure 18. Sketch of Nt on θ

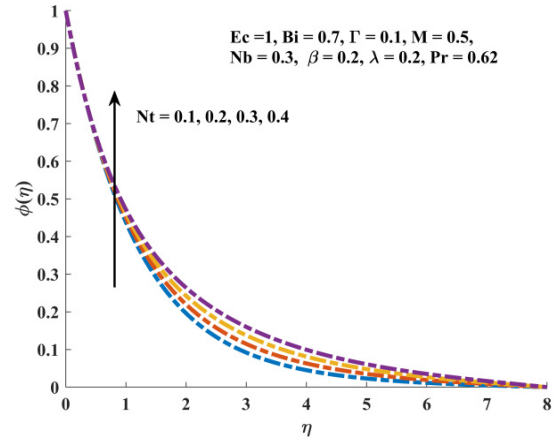

Figure 19. Sketch of Nt on ϕ

Figures 20-21 depict the impact of the Brownian motion parameter (Nb) on the both temperature and concentration profiles. In Figure 20, as enhancing in the Brownian motion parameter (Nb) the temperature profile enhances. Figure

21 illustrates how Nb impacts concentration profiles. Increasing Nb leads to reduced concentration profiles due to enhanced Brownian motion. This parameter signifies diffusion at a microscopic level, causing particles to spread out over time. Higher Nb values indicate more energetic motion, accelerating diffusion and resulting in a more uniform concentration profile. Boundary conditions, like container size and surface presence, influence particle behavior, affecting concentration profiles, particularly near solid boundaries.

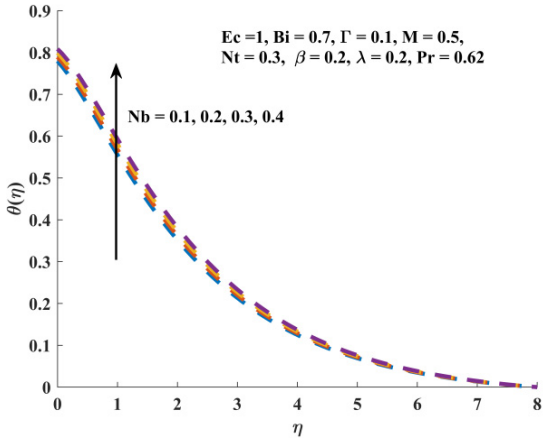

Figure 20. Sketch of Nb on θ

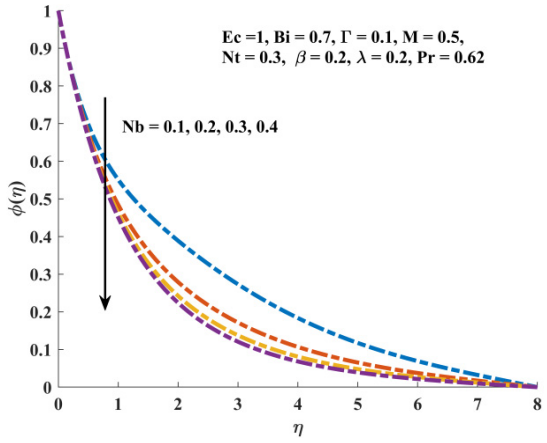

Figure 21. Sketch of Nb on ϕ

Table 1. In this section, we have to elaborate the numerical result against the different prominent factor like, $\beta = 0.2$, $\lambda = 0.2$, $Fr = 0.5$, $M = 0.5$ are the fixed values for the local skin friction coefficient. It is seemed to be as enhance in the values of Deborah number, Porosity parameter, local Forchheimer number (inertia coefficient), and Magnetic parameter, there is a decreasing nature in the skin friction coefficient.

β	λ	Fr	M	C_f
0.2				-0.217955
0.3				-0.239688
0.4				-0.261130
	0.3			-0.257903
	0.4			-0.296672
	0.5			-0.334356
		0.6		-0.243860
		0.7		-0.269300
		0.8		-0.294298
			1	-0.406792
			2	-0.724761
			3	-0.993166

Table 2. In this section, we have to elaborate the numerical result against the different prominent factor like, $\beta = 0.2$, $\lambda = 0.2$, $Fr = 0.5$, $M = 0.5$ are the fixed values for the Nusselt number. It is noticed that the Nusselt number diminishes gradually, an escalating in the values of Deborah number, Porosity parameter, local Forchheimer number (inertia coefficient), and Magnetic parameter.

β	λ	Fr	M	Nu
0.2				0.140714
0.3				0.139823
0.4				0.138949
	0.3			0.139880
	0.4			0.139062
	0.5			0.138263
		0.6		0.140584
		0.7		0.140452
		0.8		0.140318
			1	0.068228
			2	-0.049182
			3	-0.144519

CONCLUSIONS

Key findings of the study are summarized as follows.

- The velocity field diminishes for escalating the values of inertia coefficient, Magnetic parameter, Porosity Parameter, Deborah number, and also thermal relaxation parameter.
- By enhancing the values of inertia coefficient, Magnetic parameter, Porosity Parameter, Deborah number, and thermal relaxation parameter one can escalating the temperature field, but the opposite tend seen with Prandtl number.
- The concentration field increases for larger values of inertia coefficient, Magnetic parameter, Porosity Parameter, Deborah number, thermal relaxation parameter, and also for Prandtl number.
- An increment in the values of thermophoresis parameter, the temperature and concentration profiles corresponding boundary layers are upsurges gradually.
- By increasing the values of Brownian motion parameter, the temperature profile upsurges, but the reverse tend seen in the concentration profile.
- The local skin friction coefficient and Nusselt number diminishes with escalating the values of Deborah number, Inertia coefficient, Porosity, and Magnetic parameter.

ORCID

D. Dastagiri Babu, https://orcid.org/0000-0001-8114-3860; **S. Venkateswarlu**, https://orcid.org/0009-0004-8224-374X
R. Hanuma Naik, https://orcid.org/0000-0002-9817-6594

REFERENCES

[1] M.N. Khan, S. Nadeem, S. Ahmad, and A. Saleem, "Mathematical analysis of heat and mass transfer in a Maxwell fluid," Pro. I. Mech. E. Part C: J. Mech. Eng. Sci. **235**(20), 4967-4976 (2021). https://doi.org/10.1177/0954406220976704
[2] K. Sudarmozhi, D. Iranian, I. Khan, A.S. Al-johani, and S.M. Eldin, "Magneto radiative and heat convective flow boundary layer in Maxwell fluid across a porous inclined vertical plate," Sci. Rep. **13**(1), 6253 (2023). https://doi.org/10.1038/s41598-023-33477-5
[3] J. Zhao, L. Zheng, X. Zhang, and F. Liu, "Convection heat and mass transfer of fractional MHD Maxwell fluid in a porous medium with Soret and Dufour effects," Int. J. Heat Mass Tranf. **103**, 203-210 (2016). https://doi.org/10.1016/j.ijheatmasstransfer.2016.07.057
[4] T. Hayat, M. Ijaz Khan, M. Imtiaz, and A. Alsaedi, "Heat and mass transfer analysis in the stagnation region of Maxwell fluid with chemical reaction over a stretched surface," J. Therm. Sci. Eng. Appl. **10**(1), 011002 (2018). https://doi.org/10.1115/1.4024386
[5] M.B. Riaz, M. Asgir, A.A. Zafar, and S. Yao, "Combined effects of heat and mass transfer on MHD free convective flow of Maxwell fluid with variable temperature and concentration," Math. Probl. Eng. **2021**, 1-36 (2021). https://doi.org/10.1155/2021/6641835
[6] C. Bao, L. Liu, C. Xie, J. Zhu, Y. Quan, S. Chen, L. Feng, and L. Zheng, "Analysis of the absorbing boundary condition for the Maxwell fluid flow over a semi-infinite plate with considering the magnetic field," Comput Math Appl. **154**, 212-223 (2024). https://doi.org/10.1016/j.camwa.2023.11.043
[7] M. Yasin, S. Hina, and R. Naz, "A modern study on peristaltically induced flow of Maxwell fluid considering modified Darcy's law and Hall effect with slip condition," Alex. Eng. J. **76**, 835-850 (2023). https://doi.org/10.1016/j.aej.2023.06.074
[8] D. D. Babu, S. Venkateswarlu, and E. K. Reddy, "Numerical Investigation of Thermophoresis and Activation Energy Effects on Maxwell Nano Fluid Over an Inclined Magnetic Field Applied to a Disk," East Eur. J. Phys. (4), 326-335 (2023). https://doi.org/10.26565/2312-4334-2023-4-43
[9] Z. Abbas, T. Javed, N. Ali, and M. Sajid, "Flow and heat transfer of Maxwell fluid over an exponentially stretching sheet: A non-similar solution," Heat Transf-Asian Re. **43**(3), 233-242 (2014). https://doi.org/10.1002/htj.21074
[10] V. Singh, and S. Agarwal, "MHD flow and heat transfer for Maxwell fluid over an exponentially stretching sheet with variable thermal conductivity in porous medium," Therm. Sci. **18**(2), 599-615 (2014). https://doi.org/10.2298/TSCI120530120S
[11] S. Mukhopadhyay, "Heat transfer analysis of the unsteady flow of a Maxwell fluid over a stretching surface in the presence of a heat source/sink," Chin. Phys. Lett. **29**(5), 054703 (2012). https://dx.doi.org/10.1088/0256-307X/29/5/054703
[12] H. Sehra, N. Sadia, A. Z. Gul, and Z.A. Khan, "Convection heat–mass transfer of generalized Maxwell fluid with radiation effect, exponential heating, and chemical reaction using fractional Caputo–Fabrizio derivatives," Open Phys. **20**(1), 1250-1266 (2022). https://doi.org/10.1515/phys-2022-0215
[13] M. Waqas, M.M. Gulzar, W.A. Khan, M.I. Khan, and N.B. Khan, "Newtonian heat and mass conditions impact in thermally radiated Maxwell nanofluid Darcy–Forchheimer flow with heat generation," Int. J. Numer. Meth. Heat & Fluid Flow, **29**(8), 2809-2821 (2019). https://doi.org/10.1108/HFF-11-2018-0695
[14] S. Rashid, M.I. Khan, T. Hayat, M. Ayub, and A. Alsaedi, "Darcy–Forchheimer flow of Maxwell fluid with activation energy and thermal radiation over an exponential surface.," Appl. Nanosci. **10**, 2965-2975 (2020). https://doi.org/10.1007/s13204-019-01008-2
[15] H. Upreti, A. Bisht, and N. Joshi, "MHD Darcy–Forchheimer flow and double-diffusive modeling of Maxwell fluid over rotating stretchable surface: A computational study," Mod. Phys. Lett. B, **38**(27), 2450227, (2024). https://doi.org/10.1142/S0217984924502270
[16] S. Das, A. Ali, and R.N. Jana, "Darcy–Forchheimer flow of a magneto-radiated couple stress fluid over an inclined exponentially stretching surface with Ohmic dissipation," World J. Eng. **18**(2), 345-360 (2021). https://doi.org/10.1108/WJE-07-2020-0258

[17] N.V. Ganesh, A.A. Hakeem, and B. Ganga, "Darcy–Forchheimer flow of hydromagnetic nanofluid over a stretching/shrinking sheet in a thermally stratified porous medium with second order slip, viscous and Ohmic dissipations effects," Ain Shams Eng. J. **9**(4), 939-951 (2018). https://doi.org/10.1016/j.asej.2016.04.019
[18] J. Cui, A. Jan, U. Farooq, M. Hussain, and W.A. Khan, "Thermal analysis of radiative Darcy–Forchheimer nanofluid flow across an inclined stretching surface. Nanomaterials," **12**(23), 4291 (2022). https://doi.org/10.3390/nano12234291
[19] M. Jawad, and K.S. Nisar, "Upper-convected flow of Maxwell fluid near stagnation point through porous surface using Cattaneo-Christov heat flux model," Case Stud. Therm. Eng. **48**, 103155 (2023). https://doi.org/10.1016/j.csite.2023.103155
[20] A. Khan, I.A. Shah, A. Khan, I. Khan, and W.A. Khan, "Numerical investigation of MHD Cattaneo–Christov thermal flux frame work for Maxwell fluid flow over a steady extending surface with thermal generation in a porous medium," Int. J. Thermofluids, **20**, 100418 (2023). https://doi.org/10.1016/j.ijft.2023.100418
[21] K. Rubab, and M. Mustafa, "Cattaneo-Christov heat flux model for MHD three-dimensional flow of Maxwell fluid over a stretching sheet," PLoS One, **11**(4), e0153481 (2016). https://doi.org/10.1371/journal.pone.0153481
[22] A. Shahid, M.M. Bhatti, O.A. Bég, and A. Kadir, "Numerical study of radiative Maxwell viscoelastic magnetized flow from a stretching permeable sheet with the Cattaneo–Christov heat flux model," Neural Comput. Appl. **30**, 3467-3478 (2018). https://doi.org/10.1007/s00521-017-2933-8
[23] S. Islam, A. Dawar, Z. Shah, and A. Tariq, "Cattaneo–Christov theory for a time-dependent magnetohydrodynamic Maxwell fluid flow through a stretching cylinder," Adv. Mech. Eng. **13**(7), (2021). https://doi.org/10.1177/16878140211030152
[24] A. Salmi, H. A. Madkhali, B. Ali, M. Nawaz, S. O. Alharbi, and A. S. Alqahtani, "Numerical study of heat and mass transfer enhancement in Prandtl fluid MHD flow using Cattaneo-Christov heat flux theory," Case Stud. Therm. Eng. **33**, 101949 (2022). https://doi.org/10.1016/j.csite.2022.101949

ПОТІК МАГНІТОГІДРОДИНАМІЧНОЇ РІДИНИ МАКСВЕЛЛА В МОДЕЛІ ДАРСІ – ФОРХГЕЙМЕРА З ТЕПЛОВИМ ПОТОКОМ КАТТАНЕО – КРІСТОВА НАД ЛИСТОМ, ЩО РОЗТЯГУЄТЬСЯ, ЗА КОНВЕКТИВНИХ ГРАНИЧНИХ УМОВ

Д. Дастагірі Бабу[a], С. Венкатешварлу[a], Р. Ханума Наїк[b], Д. Манджула[c]
[a]Кафедра математики, Меморіальний коледж інженерії та технології Раджива Ганді, Нандьял-518501, Андхра-Прадеш, Індія
[b]Кафедра електроніки та комунікаційної техніки, Меморіальний коледж інженерії та технології Раджива Ганді, Нандьял-518501, Андхра-Прадеш, Індія
[c]Кафедра математики, Інститут інженерії та технології матері Терези, Паламанер-517408, Андхра-Прадеш, Індія

У цьому дослідницькому повідомленні досліджується потік Дарсі-Форхгеймера неньютонівської рідини Максвелла, яка хімічно реагує, над розтягнутим листом, включаючи тепловий потік Каттанео-Крістова за конвективних граничних умов. Потік рідини описується системою диференціальних рівнянь у частинних похідних, які згодом перетворюються на систему нелінійних звичайних диференціальних рівнянь. Для чисельного вирішення цих рівнянь було використано метод BVP4C після належного визначення безрозмірних змінних і реалізації перетворень подібності. Вплив різноманітних активних параметрів, таких як параметр Дебори, параметр Дарсі Форхгеймера, магнітний параметр, число Біо та параметр пористості, досліджується на профілі швидкості, температури та концентрації. Крім того, розраховані значення поверхневого тертя, та число Нуссельта представлені в табличній формі.

Ключові слова: *МГД; рідина Максвелла; модель Дарсі-Форхгеймера; тепловий потік Каттанео-Крістова; магнітний параметр*